Environmental Science & Technology

Article

Cite This: Environ. Sci. Technol. 2020, 54, 1147−1156

pubs.acs.org/est

Energy and Nutrient Recovery from Sewage Sludge and Manure via Anaerobic Digestion with Hydrothermal Pretreatment

Ci Fang,[†,§] Rixiang Huang,[†] Christy M. Dykstra,[‡] Rongfeng Jiang,[§] Spyros G. Pavlostathis,[‡] and Yuanzhi Tang*[,†,‡]

[†]School of Earth and Atmospheric Sciences, Georgia Institute of Technology, 311 Ferst Dr., Atlanta, Georgia 30332-0340, United States

[‡]School of Civil and Environmental Engineering, Georgia Institute of Technology, 311 Ferst Dr., Atlanta, Georgia 30332-0512, United States

[§]Beijing Key Laboratory of Farmland Soil Pollution Prevention and Remediation, College of Resources and Environmental Sciences, China Agricultural University, Beijing 100193, China

Supporting Information

ABSTRACT: Global expectation for sustainability has prompted the transition of practices in wastewater treatment plants toward not only waste management but also energy and nutrient recovery. It has been shown that low-temperature hydrotherm (HT) treatment can enhance downstream biogas production via anaerobic digestion (AD). Yet, because the application of combined HT and AD is still at an early stage, a systematic understanding of the dynamic speciation evolution of important elements is still lacking. This study investigates energy and nutrient recovery from sewage sludge and swine manure via combined HT-AD treatment. Bench-scale investigation was conducted to evaluate biogas production and understand the dynamic evolution of organic carbon (C) and phosphorus (P) speciation. C and P speciations were characterized using complementary chemical and spectroscopic techniques, including ^{13}C nuclear magnetic resonance (NMR) spectroscopy, P X-ray absorption near edge structure (XANES) spectroscopy, and sequential chemical extraction. Results from this study suggest that low-temperature HT pretreatment can achieve enhanced biogas production for sludge compared to the minimal effect on the biogas production from manure. It also provides guidance for P recovery from liquid digestate and solid residue after the AD process.

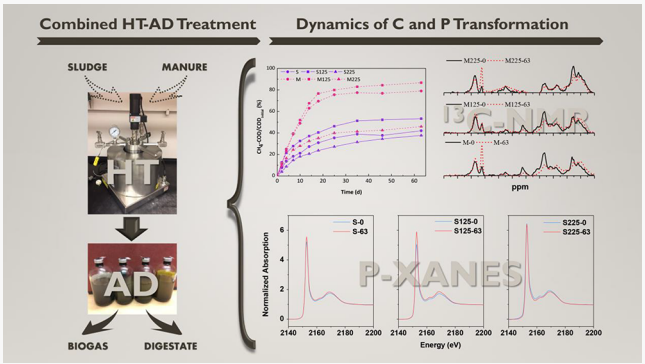

1. INTRODUCTION

Human activities lead to the production of tremendous amounts of solid biowastes, such as sewage sludge from municipal wastewater treatment plants (WWTPs) and manures from animal husbandry. For example, around 7.2 and 1.4 million tons (dry weight) of sewage sludge and animal manure, respectively, are produced annually in the US.[1,2] These biowastes contain rich amounts of organic matter and nutrients (e.g., P and N) as well as a vast variety of contaminants such as pathogens, organic pollutants, and heavy metals.[3−5] Thus, solid biowastes have great potential for energy and nutrient recovery but can also lead to serious water and soil contamination if not properly handled during treatment and/or resource recovery processes.[6−8]

Currently, the most common management strategy for sludge and manure is land application, followed by biological processing (e.g., anaerobic digestion[9,10] and composting[11,12]) and/or chemical processing (e.g., lime or alumina treatment for sanitation and P immobilization).[13−15] Although these practices can achieve certain levels of resource recovery and/or decontamination, many challenges still need to be addressed in order to improve the overall effectiveness and efficiency and to meet the growing societal pressure for sustainability. For example, the presence of extracellular polymeric substances in sewage sludge biomass can reduce the efficiency of anaerobic digestion (AD), limiting sludge methane yield to around 290−590 CH_4 mL/g-VS.[16,17] Compared to sludges, it is typically easier for animal manure to produce methane through AD, but the high concentration of ammonia in manure may inhibit the AD process[18] and the pathogens and antibiotics contained in manure cannot be fully degraded by AD.[19−22] Composting is more effective in pathogen/organic degradation than AD due to its higher treatment temperature (45−70 °C),[23,24] but the production of greenhouse gases such as CH_4 and N_2O can be problematic.[25,26] Chemical treatment methods such as lime or

Received: May 31, 2019
Revised: October 11, 2019
Accepted: December 2, 2019
Published: December 2, 2019

DOI: 10.1021/acs.est.9b03269
Environ. Sci. Technol. 2020, 54, 1147−1156

alumina addition can stabilize the wastes, with the main costs associated with the chemicals.[13−15] In addition to the above-mentioned advantages and disadvantages of conventional sludge/manure treatment methods, the final disposal of the treatment products remains challenging. For example, if the waste volume and/or pollutant contents in the final products are not significantly reduced, transportation costs and/or environmental risks of land application will remain high.

In recent years, hydrothermal treatment has emerged as a potential candidate for achieving resource recovery and decontamination of biological wastes such as sludge and manure.[27,28] Depending on the HT temperature range, the involved thermochemical reactions and product phase evolution can vary, affecting the design and selection of downstream management strategies.[29−31] It has been shown that thermal hydrolysis (i.e., temperature lower than 180 °C) can enhance downstream biogas production when the treatment products are subjected to anaerobic digestion,[32,33] while hydrothermal carbonization (i.e., temperature range of 180 to 350 °C) can facilitate sludge dewatering and increase the heating value of the products (hydrochar).[34,35] In order to achieve effective recovery of both energy (e.g., C through biogas production) and nutrients (e.g., P), it is important to understand the mass distribution and transformation of carbon and nutrients under specific treatment conditions. Yet, because the application of combined HT and AD treatment is still at an early stage, a systematic understanding of the dynamic speciation evolution of important energy and nutrient elements is still lacking.

To fill the above-mentioned knowledge gap, this study systematically investigated the effects of hydrothermal pretreatment (at 125 and 225 °C) on the AD of sewage sludge and swine manure, with a focus on the dynamic evolution of organic matter and phosphorus during the combined treatment process. Carbon speciation in the liquid and solid phases was probed by the evolution of chemical oxygen demand (COD) and ^{13}C nuclear magnetic resonance (NMR) spectroscopy, while phosphorus speciation was characterized by P K-edge X-ray absorption near edge structure (XANES) spectroscopy. To our knowledge, this is the first study that systematically investigates the fundamental processes underlying carbon and phosphorus transformation during combined hydrothermal treatment and anaerobic digestion and provides a valuable basis for the design and optimization of this technology for effective energy and nutrient recovery.

2. MATERIALS AND METHODS

2.1. Collection and Hydrothermal Treatment of Sludge and Manure Samples. Activated sludge was collected from the secondary treatment tank from a local WWTP in Atlanta, Georgia, U.S.A.. After collection, sludge was allowed to settle and the supernatant was discarded. Swine manure was collected from a local farm in the vicinity of Atlanta, Georgia, U.S.A.. The water content of the sludge and manure was 88% and 78.9%, respectively. A 1:5 (w/w) solid to liquid ratio was used for hydrothermal treatment. Specifically, 12 g of sample and an appropriate amount of deionized water (DI) were added into a 20 mL Teflon lined stainless steel hydrothermal reactor (Parr instrument). The reactor was sealed and heated in an oven at 125 or 225 °C for 4 h and then allowed to cool to 50 °C overnight in an oven. Raw sludge, manure, and their hydrothermally derived hydrochars were stored at 4 °C for less than a week before anaerobic digestion.

2.2. Anaerobic Digestion. Anaerobic digestion (AD) was conducted on seven sets of feedstocks: control (CK), sludge (S), manure (M), and their hydrochars derived by HT at 125 or 225 °C (S125, S225, M125, and M225). AD was carried out in 160 mL serum bottles (with 100 mL liquid volume), and each set was performed in quadruplicate. Anaerobic sludge obtained from the mesophilic anaerobic digester of the same WWTP was anaerobically preincubated in the laboratory and served as the seed inoculum. The serum bottles were capped with rubber stoppers and flushed with nitrogen gas. Twenty milliliter of DI water (CK), sludge (S), manure (M), or their hydrochars (S125, S225, M125, or M225) were first added to the bottles. Then, 50 mL of the seed inoculum was anoxically transferred to each bottle, followed by the addition of 30 mL of anoxic medium. The medium contained: 0.9 g/L K_2HPO_4, 0.5 g/L KH_2PO_4, 0.5 g/L NH_4Cl, 0.1 g/L $CaCl_2{\cdot}2H_2O$, 0.2 g/L $MgCl_2{\cdot}6H_2O$, 0.1 g/L $FeCl_2{\cdot}4H_2O$, and 3.5 g/L $NaHCO_3$. Stock solutions of 1 g/L resazurin, vitamin, and trace metals were each added to the medium to achieve a final concentration of 1.0 mL/L. Quadruplicate bottles were used for each set, with one bottle stored at 4 °C as 0 day sample and the other three bottles incubated in the dark at 35 °C for AD process, shaken manually twice a day. Throughout the incubation period of 63 days, total gas volume and composition (CH_4 and CO_2) were measured every 2−4 days during the first 20 days and every 7−14 days afterward. At the end of the incubation period, the pH, total and volatile solids (TS, VS), total chemical oxygen demand (TCOD), soluble chemical oxygen demand (SCOD), total P (TP), soluble P (IP), and ammonia (NH_4^+) were measured.

TS, VS, pH, TCOD, SCOD, TP, IP measurements were conducted according to procedures described in Standard Methods.[36] Total nitrogen (TN) and total carbon (TC) were measured using a Carlo Erba CHN analyzer.[37] Total gas production was measured by displacement of an acidified brine solution (10% NaCl w/v and 2% H_2SO_4 v/v) in graduated burets. The gas composition was determined by gas chromatography with thermal conductivity as previously reported.[38,39]

2.3. ^{13}C NMR Analysis. Sludge, manure, and their hydrochars before and after 63 d AD were freeze-dried and analyzed by ^{13}C solid-state NMR spectroscopy to investigate the change of C speciation during anaerobic digestion. Sample powders were tightly packed into a cylindrical zirconia rotor (4 mm O.D.) with a Kel-F cap. NMR data were collected on a Bruker Avance III 400 spectrometer equipped with a 4 mm probe. A ramp cross-polarization (ramp-CP) pulse program (where the proton contact pulse was ramped from 50 to 100% and that of carbon was fixed) coupled with magic angle spinning (MAS) was used.[40] The spectra were obtained at 100.570 MHz, a contact time of 3 ms, a recycle delay of 4 s, and sample spinning rate at 12 kHz. A total of 4096 scans were collected for each sample. Spectral processing and analysis were carried out using Bruker TopSpin 3.5 (Bruker Inc., Billerica, MA, U.S.A.). Assignment and quantification of C functional groups were based on Vane et al. (2005),[41] with the following groups identified: (1) aliphatic (chemical shift of 0−50 ppm), (2) methoxyl (50−60 ppm); (3) O/N-alkyl (60−110 ppm); (4) aromatic, furanic, and O-aromatic (110−160 ppm), and (5) carboxyl and carbonyl (160−210 ppm) (details in Table S1).

2.4. Sequential Chemical Extraction. Sequential chemical extraction was conducted on the raw and treated samples

DOI: 10.1021/acs.est.9b03269
Environ. Sci. Technol. 2020, 54, 1147−1156

Table 1. Characteristics of Sludge, Swine Manure, and Their Hydrothermally Treated Samples at 125 or 225 °C[b]

Parameter[a]	Sludge	S125	S225	Manure	M125	M225
TS (%)	9.51 ± 0.03	8.91 ± 0.07	7.86 ± 0.19	17.63 ± 0.07	16.53 ± 0.04	11.56 ± 0.42
VS (%)	7.26 ± 0.22	6.48 ± 0.25	4.52 ± 0.31	15.49 ± 0.46	14.81 ± 0.34	9.44 ± 0.55
pH	6.65 ± 0.04	6.10 ± 0.02	7.75 ± 0.01	6.50 ± 0.06	5.64 ± 0.04	5.36 ± 0.01
TCOD (g/L)	99.4 ± 0.2	100.0 ± 0.2	111.4 ± 0.2	134.7 ± 0.1	139.0 ± 0.1	210.0 ± 0.1
C content (wt%)	35.70 ± 0.13	36.08 ± 0.20	37.78 ± 0.30	41.18 ± 0.99	41.89 ± 0.64	53.15 ± 1.84
N content (wt%)	7.14 ± 0.03	7.17 ± 0.06	6.78 ± 0.14	3.63 ± 0.02	4.16 ± 0.26	4.73 ± 0.09
C/N ratio	5.00	5.03	5.57	11.34	10.07	11.24
Total P (mg/g dt)	56.21 ± 0.85			23.10 ± 0.28		
Cu (mg/kg dt)	27.55 ± 0.29			16.39 ± 0.22		
Zn (mg/kg dt)	77.36 ± 0.41			102.91 ± 1.61		
Cr (mg/kg dt)	12.89 ± 0.33			8.57 ± 0.28		
As (mg/kg dt)	8.79 ± 0.26			6.29 ± 0.13		
Cd (mg/kg dt)	1.64 ± 0.03			0.48 ± 0.01		

[a]TS (total solids), VS (volatile solids), TCOD (total chemical oxygen demand), dt (dry weight). Data error bars represent mean ± standard deviation (n = 3). [b]Labeled as S125 and S225 for sludge and M125 and M225 for manure.

following the Hedley's method[42] to assess P speciation. The extraction method considers the P species extracted by H_2O, $NaHCO_3$, NaOH, and HCl to be readily soluble P, exchangeable P, Fe/Al mineral adsorbed P, and insoluble phosphates, respectively. Specifically, 100 mg raw sludge, manure, or their corresponding hydrochars were added to a 50 mL polypropylene centrifuge tube and sequentially extracted by 20 mL extraction solutions. The reaction tubes were constantly agitated by end-to-end shaking. The samples were first extracted with DI water for 8 h, followed by 0.5 M $NaHCO_3$, 0.1 M NaOH, and 1.0 M HCl solutions, each lasting 16 h. All experiments were conducted in duplicate. At the end of each extraction step, the solid and aqueous phases were separated by vacuum filtration (0.45 μm). The filtrate was digested using the persulfate digestion method[36] and analyzed for P concentration using the phosphomolybdate colorimetric assay[43] on an UV−vis spectrometer (Carey 60, Agilent).

2.5. P K-edge XANES Analysis. P K-edge XANES data were collected at Beamline 14−3 at the Stanford Synchrotron Radiation Lightsource (SSRL), Menlo Park, CA. Samples before and after AD treatment were freeze-dried, ground into fine powders, and brushed evenly onto P-free Kapton tapes. Excess powders were blown off to achieve a homogeneous and thin film. Sample-loaded tapes were mounted to a sample holder. The sample chamber was maintained under a He atmosphere at room temperature. XANES data were collected in fluorescence mode using a PIPS detector at 2100−2485 eV. Multiple scans were collected for each sample, energy calibrated, merged, and normalized for further analysis. Principle component analysis (PCA) and linear combination fitting (LCF) was conducted at an energy range of −15 to +50 eV. E_0 values of reference compounds were allowed to float for up to ±1 eV. Goodness of fit was evaluated using the residual factor (R factor), and the fit with lowest R factor was used. Because Fe, Al, and Ca are the predominant metals present in sludge and manure, phosphate could either adsorb on their mineral phases or form solid precipitates with them. Therefore, XANES data were also collected on the following reference compounds for LCF: (1) amorphous calcium phosphate (ACP) and hydroxyapatite (HAP), representing Ca-associated P; (2) $AlPO_4$ and phosphate sorbed on γ-alumina, representing Al-associated P; (3) phosphate sorbed on ferrihydrite (P-Ferrihy), representing Fe-associated P; (4) phytic acid (PhyAc, sodium salt), representing P associated with organic functional groups. Synthesis of the reference compounds, their P XANES spectra, and details of LCF can be found in our previous study.[28]

2.6. Statistical Methods. One-way analysis of variance (ANOVA) was performed to compare results from different treatments. Significant differences were determined according to a Tukey HSD test at a significance level of 0.05. All statistical tests were performed using JMP software (Version 10, SAS Institute Inc., Cary, NC, U.S.A.).

3. RESULTS AND DISCUSSION

3.1. Physicochemical Characteristics of AD Feedstocks. The physicochemical characteristics of sludge, manure, and their HT treated products are shown in Table 1. Generally, both total and volatile solids decreased after HT at increasing temperatures, due to the increasing solubilization and volatilization of organic matter into liquid and gas phases, respectively. The pH value decreased to 6.10 at 125 °C but increased to 7.75 at 225 °C for HT treated sludge, while pH decreased from 5.64 at 125 °C to 5.36 at 225 °C for HT treated manure. TCOD for both sludge and manure samples increased after HT (particularly at 225 °C), likely due to dehydration and decarboxylation during HT that reduces oxygen content in the biomass.

3.2. Energy Recovery: Transformation of Organic Matter. Biogas production was monitored for a 63 day period, and the effects of HT on biogas production kinetics and extent were evaluated and related to the form of organic matter in the feedstock. Cumulative biogas production showed a rapid increase during the initial 20 days, followed by a near steady rate (Figure S1). Both 125 and 225 °C HT treatments enhanced total gas and CH_4 per VS compared to raw materials. For manure samples, the effect of HT on gas production was more pronounced by 125 °C treatment, with methane production (over 700 mL/g VS) significantly higher than the 225 °C treatment in this study (Table S2) or other previous results.[44,45]

In order to analyze the relationship between methane production and COD removal potential after HT and AD processes, methane production was expressed by equivalent COD consumption (CH_4-COD). Under standard temperature and pressure, 1 g of COD is consumed to produce 350 mL methane, so the methane production volume of 1 g of COD under different temperatures can be calculated as follows,

DOI: 10.1021/acs.est.9b03269
Environ. Sci. Technol. 2020, 54, 1147−1156

$$\text{CH}_4\text{-COD (mg/L)} = \frac{1000 \times V_{CH_4}}{\left(350 \times \frac{273.15 + T}{273.15}\right) \times V} \quad (1)$$

where V_{CH_4} is the total volume of biogas (mL), T is the temperature of AD treatment (K), and V is the total volume of AD samples (L). For better comparison, methane production from each experimental series was normalized to initial substrate COD and the results are shown in Figure 1 and

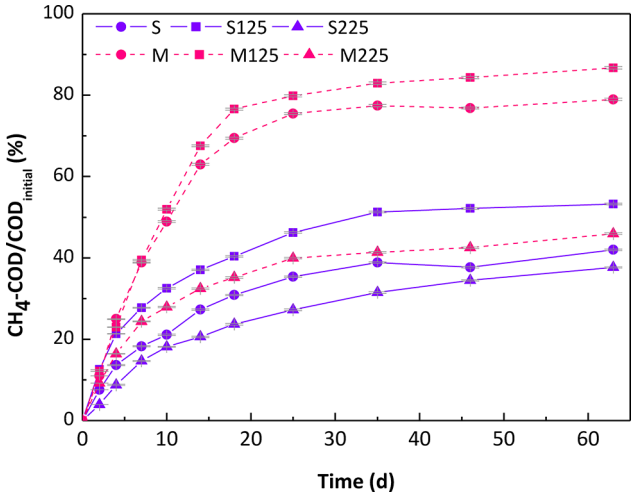

Figure 1. Cumulative methane production in ultimate digestibility experimental series, normalized to the initial total substrate COD. Error bars represent mean values ± one standard deviation (n = 3).

Table S3. The COD destruction ($\text{COD}_{\text{destroy}}$) agrees well with the conversion of the initial substrate COD to methane ($\frac{\text{CH}_4\text{-COD}}{\text{COD}_{\text{initial}}}$). After this normalization, for both sludge and manure samples, the total gas and methane productions were enhanced by the 125 °C HT treatment but inhibited by the 225 °C treatment. Indeed, HT treatments above 180 °C have been previously reported to inhibit CH_4 production in downstream AD.[46−51] At high temperatures, Maillard reaction can occur between amino acids and reducing sugars, which produces recalcitrant products (e.g., melanoidin) that are less bioavailable for biogas production and may act as microbial inhibitors.[48−50,52] In one study, Maillard reaction products were identified in the liquid fraction of sludge following HT treatment at temperatures from 180 to 200 °C;[50] thus, it is likely that the 225 °C HT treated sludge and manure in the present study contained Maillard reaction products. Higher temperatures could also lead to the loss of volatile fatty acids (VFAs) through volatilization, thereby decreasing available substrate for biogas production.[48,50] Furthermore, high HT temperatures could lead to high liquid-phase concentrations of VFAs and/or long chain fatty acids (LCFAs) that can inhibit AD.[50,51] Ammonia, which is released during the thermal hydrolysis of proteins, can also be inhibitory to AD.[47,50,53] In the present study, AD produced ammonia concentration ranged from 171 to 251 mg-N/L initially and 227 to 297 mg-N/L at the end of incubation. Unacclimated AD systems can be completely inhibited at 1700 mg-N/L to 1800 mg-N/L, although acclimated systems can withstand total ammonia concentrations up to 5000 mg-N/L before complete inhibition.[53]

Anaerobic digestion of complex particulate organic matter is a multistep process involving series and parallel reactions, typically grouped into four subprocesses: hydrolysis, acidogenesis, acetogenesis, and methanogenesis.[54,55] The kinetics of anaerobic digestion have been described by various models.[54,56] In this study, the pseudo first-order kinetics model was used to assess the overall digestibility of these samples during the batch assay, as follows,

$$\frac{S_t}{S_u} = 1 - e^{-kt} \quad (2)$$

where S_t is the concentration of degradable substrate converted to methane at time t (mg COD/L), S_u is the concentration of ultimately degradable substrate converted to methane (mg COD/L), k is the pseudo first-order rate constant (d^{-1}), and t is the incubation time (d). The fitting results are shown in Figure S2 and Table 2. All the data can be well fitted by the

Table 2. Pseudo First-Order Rate Constants for the Conversion of Degradable COD to Methane for Sludge (S), Manure (M), and Their Hydrothermal Treated Samples at 125 or 225 °C

Sample	Rate constant (k, d^{-1})[a]	R^2
Sludge	0.076 ± 0.003	0.982
S125	0.095 ± 0.006	0.969
S225	0.058 ± 0.002	0.987
Manure	0.103 ± 0.004	0.991
M125	0.095 ± 0.004	0.987
M225	0.094 ± 0.005	0.973

[a]Mean estimate ± standard error ($n \geqslant 6$).

pseudo first-order kinetic model with R^2 values over 0.96. The rate constant (k) for the anaerobic digestion of all sludge samples decreased in the following order: S125 > S > S225, but it did not vary significantly for all manure samples (ranging from 0.094 to 0.103 d^{-1}). This suggests that for sludge samples, the 125 °C HT treatment enhanced not only the extent of biogas production but also the production rate, whereas the biogas production rate for manure samples was not affected by HT regardless of treatment temperature.

Solid-state ^{13}C NMR analysis was used to characterize the structural transformation of insoluble organic matter during the HT and AD processes (Figure 2, Tables S4 and S5). A broad band located at a 0−50 ppm chemical shift with two peaks centered at ∼25 and 30 ppm (signals from alkyl carbons) suggests the presence of humic substances, lipids, cutin-like structures, and other aliphatic biomolecules.[57,58] The peak at around 56−57 ppm is assigned to methoxy groups, indicating the presence of lignin-like structures.[59,60] The region at 60−110 ppm is assigned to oxygen- or nitrogen-substituted alkyl carbons (O/N-alkyl), suggesting the presence of carbohydrates and cellulose.[61,62] The aromatic carbon spectral region is represented at 110−160 ppm, and the small peaks at 130 and 137 ppm correspond to *p*-hydroxyphenol derivatives and aromatic rings, respectively.[41,62] The region at 160−210 ppm shows a mixture of carboxylic, amide, and ester groups with strong peaks at ∼168 ppm (i.e., hydroxyls) and 174 ppm (i.e., carboxyls).[12] The generation of this region is consistent with the oxidative degradation of organic matters.

It is clear that sludge has high contents of alkyl, carboxyl, and carbonyl groups, with two dominant broad bands at 0−50 ppm and 160−210 ppm in the ^{13}C NMR spectra (Figure 2I),

DOI: 10.1021/acs.est.9b03269
Environ. Sci. Technol. 2020, 54, 1147−1156

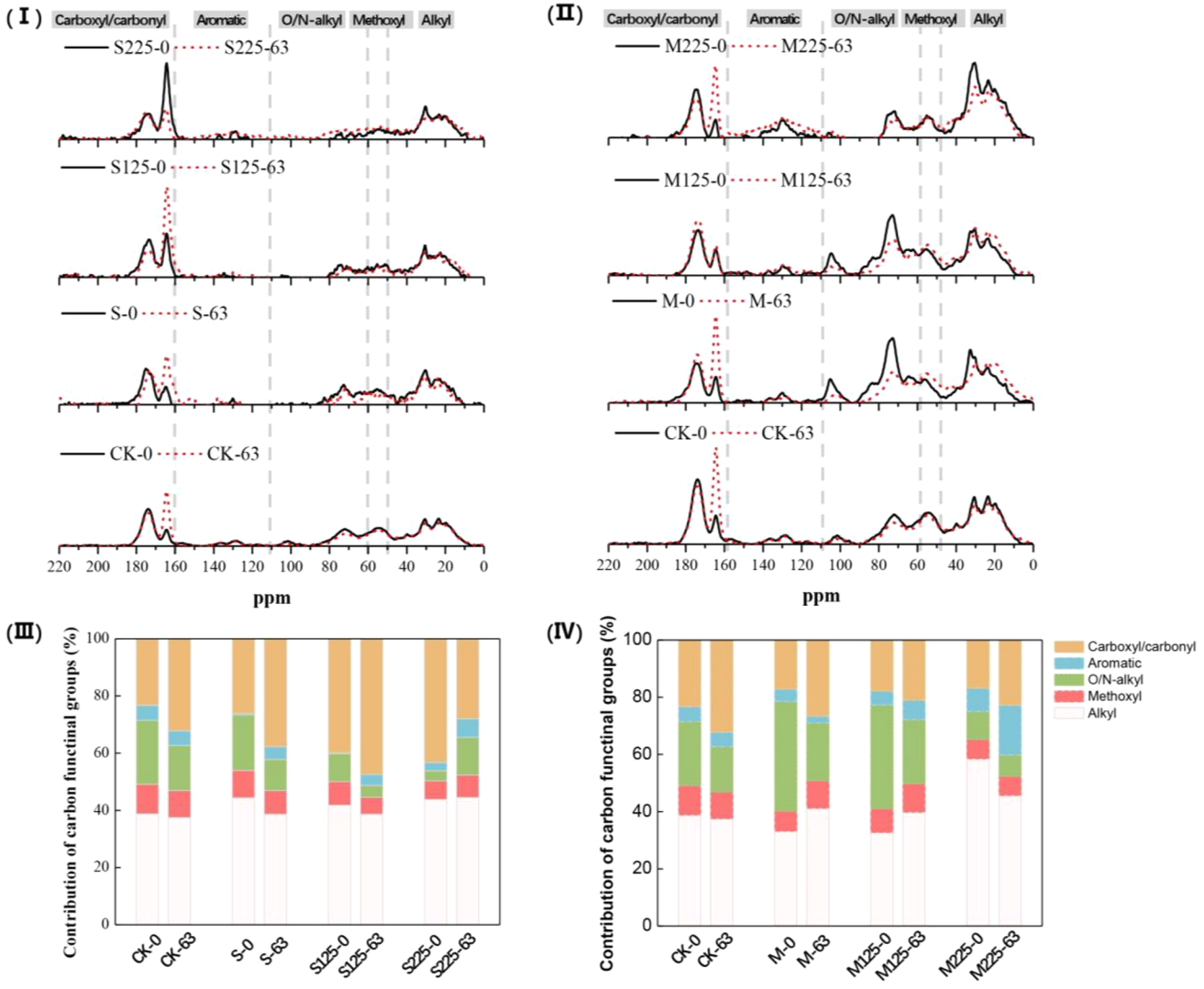

Figure 2. (I) ^{13}C solid-state NMR spectra of DI water (CK), raw sludge (S), and sludge hydrochars (S125 and S225) at day 0 (labeled as 0) and day 63 (labeled as 63) of anaerobic digestion. (II) ^{13}C solid-state NMR spectra of DI water (CK), raw manure (M), and manure hydrochars (M125 and M225) at day 0 and 63 of anaerobic digestion. (III) Contribution of different carbon functional groups derived from the NMR spectra in panel I, expressed as the peak area ratio between each functional group and the total peak area. (IV) Contribution of different carbon functional groups derived from the NMR spectra in panel II.

while manure has high O/N-alkyl content, with a broad band at 60−110 ppm, likely associated with the presence of cellulose carbons with signals at 65 ppm (C-6), 73 ppm (C-2, C-3, C-5), and 82 ppm (C-4 in amorphous cellulose, hemicellulose, and cellulose oligomers), as well as anomeric carbon in cellulose at 105 ppm.[62] The difference in organic composition between raw sludge and manure is due to their origination. For animal manures, dietary composition, animal physiology, and manure handling process would determine the organic composition, which includes protein, lipids, and undigested carbohydrates.[63,64] For sludge, microbial biomass and thus more cellular structures is more likely to appear, regardless of different wastewater treatment methods or subsequent handling processes.[65]

After HT treatment, for sludge samples, the contributions from methoxy (50−60 ppm) and O/N-alkyl (60−110 ppm) groups decreased and those from the aromatic (110−160 ppm) and carboxyl and carbonyl (160−210 ppm) groups increased significantly. Specifically, the contribution of O/N-alkyl decreased from 19.4% to 3.6% and that of the aromatic groups increased from 0.5% to 2.9% in S225, and carboxyl and carbonyl groups increased from 26.1% to 39.8% in S125, suggesting a high degree of polyphenolic polycondensation rather than ring cleavage of polyphenolic entities.[66] For manure samples, HT at 225 °C decreased the contribution of O/N-alkyl group from 38.4 to 9.8% with the increase of alkyl and aromatic signals, suggesting that aliphatic chains and carbohydrates in the manure were converted partly to polycyclic aromatic groups and partly to shorter alkyl moieties under higher temperature HT treatment.[67] All the results indicated that HT treatment is a process of deoxygenation and upgrading, with more obvious effects at higher treatment temperature.[58]

After the AD process, the aromatic groups increased in both the sludge and manure samples with the decrease of O/N-alkyl, except for sample S225. A combination of the SCOD results in Table S6 shows that it is possible that the relative increase of aromatic group is partly due to the decrease of O/N-alkyl, long chain carboxyl, and carbonyl groups with the fast degradation of solid organics during AD, and partly due to the

DOI: 10.1021/acs.est.9b03269
Environ. Sci. Technol. 2020, 54, 1147−1156

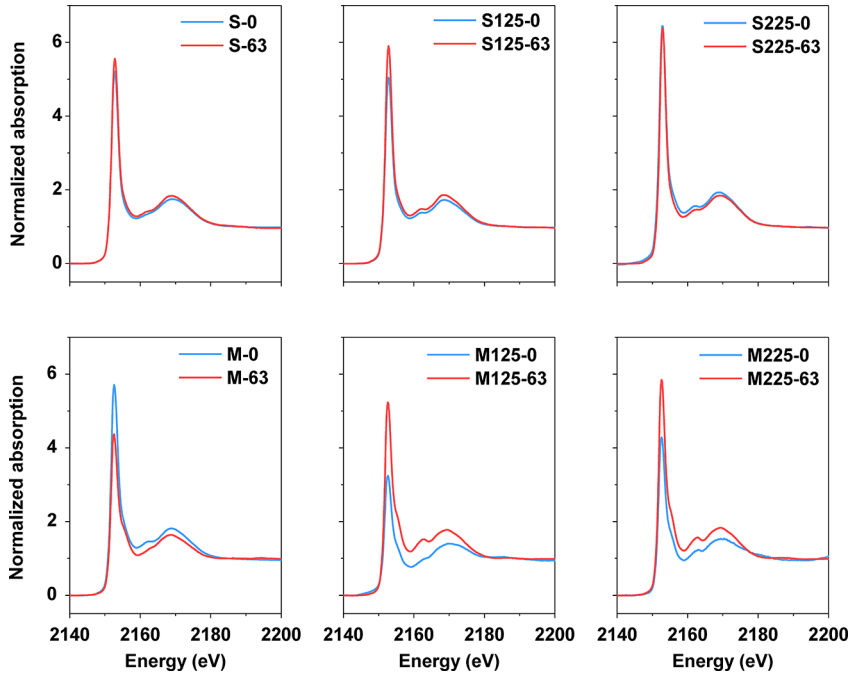

Figure 3. Normalized results of P XANES spectra of sludge, manure, and their hydrochars at day 0 (labeled as 0) and day 63 (labeled as 63) of anaerobic digestion. Fitting results are in Table 3.

Table 3. Relative Abundance and R Factors of Different P Species Determined by Linear Combination Fitting (LCF) of P XANES Spectra of DI Water (CK), Sludge, Manure, and Their Hydrothermally Treated Samples before (labeled as 0) and after (labeled as 63) Anaerobic Digestion[a]

	Relative abundance (%)						
Sample	ACP	HAP	$AlPO_4$	P-Alumina	P-Ferrihy	PhyAc	R factor
CK-63	42.2		57.8				0.00639
S-0	38.9		30.2			30.9	0.00291
S-63	33.6		37.0			29.4	0.00153
S125-0	40.6		20.4		11.3	27.7	0.00093
S125-63	31.2		25.2		20.4	23.2	0.00110
S225-0		23.5	10.2	48.0	18.3		0.00120
S225-63		30.2	28.8	21.2	19.8		0.00051
M-0	32.5		34.4			33.1	0.00515
M-63	77.8					22.2	0.00304
M125-0		46.8	53.2				0.03873
M125-63		70.1	29.9				0.00249
M225-0		60.4	29.8	9.8			0.00508
M225-63		58.4	21.3	20.3			0.00163

[a]Raw spectra are shown in Figure 3 and Figure S4.

recombination of alkyl. For sample S225, the increase of O/N-alkyl might come from soluble organics due to microbial metabolisms, which might be the compounds that inhibited methane formation (e.g., furfural, hydroxyl methyl furfural (HMF) groups).[68,69] Previous studies reported that furfural and HMF concentrations in the HT-biomass over 200 °C were higher than the threshold inhibitory concentration, which might lead to moderate or complete inhibition of specific methanogenic activity.[70,71] However, these explanations warrant future investigations.

Overall, HT pretreatment enhanced the release of organics in sludge and improved the degradation of organics in manure during AD process. After both HT and AD treatments of sludge samples, more O/N-alkyl was continuously converted to carboxyl, carbonyl, and soluble organics. For manure samples, HT-AD converted soluble organics and O/N-alkyl partly to carboxyl and carbonyl and partly to alkyl at the same time. In combination with the trends in gas production, the 125 °C HT pretreatment seems to be more suitable than the 225 °C treatment for both sludge and manure from the aspect of biogas production (i.e., energy recovery).

3.3. Nutrient Recovery: P Phase Distribution. The phase distribution of P strongly affects the strategy and efficiency of P recovery from the treatment products. Therefore, the distribution of P in the liquid (digestate) and solid phases after both HT and HT-AD was evaluated (Table S7). Because of the high P content in the medium, the content of liquid-TP was overall high. However, with the addition of feedstock, the ratio of liquid-TP decreased from 86.7% to 60–78%. The liquid-TP slightly increased after AD, except for

DOI: 10.1021/acs.est.9b03269
Environ. Sci. Technol. 2020, 54, 1147−1156

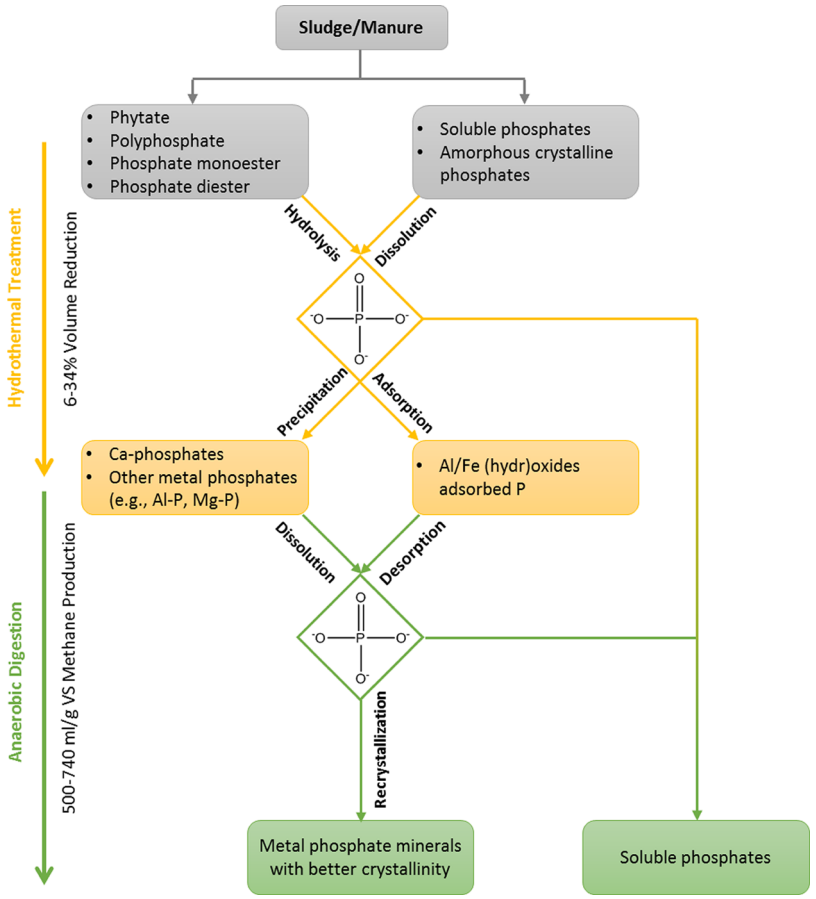

Figure 4. Schematic illustration of the proposed mechanisms involved in the transformation of P during hydrothermal treatment and anaerobic digestion of sludge and manure.

sample S225. Both microbiological and physicochemical mechanisms might have accounted for the release of P.[72,73] The decreased content of liquid-TP after AD in sample S225 might be related to the decreasing content of SCOD after AD (Table S6), as P can coprecipitate with the recombination of particle organics, which was discussed in the section Energy Recovery: Transformation of Organic Matter.

From a nutrient recovery aspect, P reclamation might be directly conducted for the digestate via the precipitation of P-containing minerals such as struvite. In our set up, after the combined HT-AD treatment, pH values of all samples were at ~8, an optimal range for struvite precipitation.[74] The content of Mg, a component element of struvite, was also enriched after the AD process (Table S7). Considering the stoichiometry of struvite (Mg/N/P = 1:1:1) and the relatively lower molar ratio of Mg in the digestate as compared to P and N, more Mg needs to be added to increase the supersaturation for struvite precipitation.[75]

3.4. Nutrient Recovery: P Speciation Transformation in the Solid Products. Since the mobility and phase migration behavior of P are largely controlled by its speciation, P speciation in the raw sludge/manure, their HT treatment products, and the HT-AD treatment products was characterized by combining sequential chemical extraction and P XANES analysis (Figure 3, Table 3, and Figure S3).

Linear combination fitting of P XANES data showed that amorphous calcium phosphate (ACP; 38.9% and 32.5% for sludge and manure, respectively), $AlPO_4$ (30.2% and 34.4% for sludge and manure, respectively), and phytate (PhyAc; 30.9% and 33.1% for sludge and manure, respectively) were the three main species in both raw sludge and manure. After both 125 and 225 °C HT treatments, transformation of ACP to hydroxyapatite (HAP) and decrease of phytate were observed in both sludge and manure hydrochars, suggesting the degradation of organics and increased crystallinity of calcium phosphate phase(s).[45] In addition, Fe-associated P existed as ferrihydrite adsorbed P (P-Ferrihy) in HT treated sludge samples and the relative abundance of P-Ferrihy increased with increasing HT temperature. The Al-associated P existed as $AlPO_4$ and P-Alumina (alumina adsorbed P) after the 225 °C HT treatments for both sludge and manure.

P sequential extraction results also showed the decrease of water-soluble inorganic P (IP) and increase of HCl-extractable IP in both sludge and manure following the HT treatment. HCl-extractable IP is operationally categorized as insoluble, low mobility phosphate phases such as calcium phosphate and $AlPO_4$. Most of the IP in the sludge was extracted by 0.1 M NaOH (i.e., Fe/Al mineral adsorbed P). These results were generally consistent with the P XANES analysis and indicated the low bioavailability of P after HT treatment.[28,29] The P speciation change during HT is controlled by the composition and states of metal cations with high affinity for phosphate as well as the thermochemical reactions that occurred during HT process. During HT treatment, reactions such as hydrolysis, decarboxylation, and polymerization were found to be involved in the transformation of biomass.[76] These reactions were responsible for the hydrolysis of polyphosphate into orthophosphate for sludge and manure and can expose the

DOI: 10.1021/acs.est.9b03269
Environ. Sci. Technol. 2020, 54, 1147−1156

intracellular and organic-bound P to metals such as Ca, Al, and Fe.[77] This can explain the decrease of phytate and the increase in Ca−P crystallinity after HT treatment.

After the 63 day AD treatment (Table 3), the relative abundances of ACP and PhyAc in samples S and S125 decreased, accompanied by increases in $AlPO_4$ and P-Ferrihy. The relative abundance of Ca-associated P (include ACP and HAP) increased in M and M125 with the decrease of $AlPO_4$ and PhyAc. There were no obvious changes of P speciation in both S225 and M225 before and after AD treatment. Contrary to the changes of P speciation before and after HT treatment, there was little change in the relative abundance of different P species before and after AD. Since P in HT samples has been relatively homogenized, especially under the 225 °C HT treatment, the magnitude of alterations (changes in only the relative abundance of P speciation) was much smaller. In general, Ca/Fe/Al-associated P species (e.g., mineral adsorbed or precipitated) are more stable than Na/K/Mg-associated P species. In addition, the decreasing content of PhyAc after HT treatment suggests the decreased association of P with organics. Although some P came from CK and the relative abundance of P speciation could be fitted successfully only from the 63 day CK sample (Table 3 and Figure S4), the results indicated that ACP and $AlPO_4$ were the main species in the medium and seed after AD. CK might have little effect on the overall P transformation mechanism during the HT and AD combined treatments, but further studies are warranted to investigate the effect of medium addition (and nutrient supply) on the performance and element evolution of the whole system.

Overall, P species in the solid products after the HT-AD treatments experienced improved crystallinity. As summarized in Figure 4, under HT conditions, orthophosphates derived from organophosphates or polyphosphate can become available for the formation of phosphate precipitates or adsorption to minerals,[77] and the formed species may dissolve/desorb and reorganize/recrystallize to generate higher crystallinity phosphate salts after the AD process.

■ ASSOCIATED CONTENT

Supporting Information

The Supporting Information is available free of charge at https://pubs.acs.org/doi/10.1021/acs.est.9b03269.

^{13}C NMR spectra; analysis of biogas production; batch ultimate digestibility test results; percent contribution of carbon functional groups; characteristics of organic contents of sludge, manure, and their hydrochars; solution concentrations of total P (liquid-TP), ammonia, and Mg; cumulative total gas, methane, and carbon dioxide production; normalized methane COD production; relative percentage of P species in each sequential extraction step (color bars) and the total P content (open symbol) in sludge, manure, and their hydrothermally treated samples; normalized P XANES spectra of DI water sample (PDF)

■ AUTHOR INFORMATION

Corresponding Author

*Tel: 404-894-3814. E-mail: yuanzhi.tang@eas.gatech.edu.

ORCID

Christy M. Dykstra: 0000-0002-1469-5072

Spyros G. Pavlostathis: 0000-0001-9731-3836

Yuanzhi Tang: 0000-0002-7741-8646

Notes

The authors declare no competing financial interest.

■ ACKNOWLEDGMENTS

This work is supported by the U.S. National Science Foundation (NSF) under Grant numbers 1739884, 1559087, and 1605692. C. Fang acknowledges support from China Scholarship Council. We appreciate the help from beamline scientist Matthew Latimer at SSRL Beamline 14-3 for help with experimental setup and data collection. Portions of this research were conducted at the Stanford Synchrotron Radiation Lightsource (SSRL). SSRL is a Directorate of SLAC National Accelerator Laboratory and an Office of Science User Facility operated for the U.S. Department of Energy Office of Science by Stanford University.

■ REFERENCES

(1) Peccia, J.; Westerhoff, P. We should expect more out of our sewage sludge. *Environ. Sci. Technol.* **2015**, *49* (14), 8271−8276.

(2) He, Z.; Pagliari, P. H.; Waldrip, H. M. Applied and environmental chemistry of animal manure: A review. *Pedosphere* **2016**, *26* (6), 779−816.

(3) Venglovsky, J.; Sasakova, N.; Placha, I. Pathogens and antibiotic residues in animal manures and hygienic and ecological risks related to subsequent land application. *Bioresour. Technol.* **2009**, *100* (22), 5386−5391.

(4) Ji, X.; Shen, Q.; Liu, F.; Ma, J.; Xu, G.; Wang, Y.; Wu, M. Antibiotic resistance gene abundances associated with antibiotics and heavy metals in animal manures and agricultural soils adjacent to feedlots in Shanghai; China. *J. Hazard. Mater.* **2012**, *235*, 178−185.

(5) Ignatowicz, K. The impact of sewage sludge treatment on the content of selected heavy metals and their fractions. *Environ. Res.* **2017**, *156*, 19−22.

(6) Kleinman, P. J.; Sharpley, A. N.; Wolf, A. M.; Beegle, D. B.; Moore, P. A. Measuring water-extractable phosphorus in manure as an indicator of phosphorus in runoff. *Soil Sci. Soc. Am. J.* **2002**, *66* (6), 2009−2015.

(7) Cordell, D.; Drangert, J.-O.; White, S. The story of phosphorus: Global food security and food for thought. *Global Environmental Change* **2009**, *19* (2), 292−305.

(8) Steele, K. F. *Animal waste and the land-water interface*. Lewis Publishers: 1995.

(9) Hartmann, H.; Ahring, B. K. Anaerobic digestion of the organic fraction of municipal solid waste: influence of co-digestion with manure. *Water Res.* **2005**, *39* (8), 1543−52.

(10) Kim, J. K.; Oh, B. R.; Chun, Y. N.; Kim, S. W. Effects of temperature and hydraulic retention time on anaerobic digestion of food waste. *J. Biosci. Bioeng.* **2006**, *102* (4), 328−32.

(11) Tang, J.-C.; Maie, N.; Tada, Y.; Katayama, A. Characterization of the maturing process of cattle manure compost. *Process Biochem.* **2006**, *41* (2), 380−389.

(12) Jouraiphy, A.; Amir, S.; Winterton, P.; El Gharous, M.; Revel, J. C.; Hafidi, M. Structural study of the fulvic fraction during composting of activated sludge-plant matter: elemental analysis, FTIR and ^{13}C NMR. *Bioresour. Technol.* **2008**, *99* (5), 1066−72.

(13) Kalbasi, M.; Karthikeyan, K. G. Phosphorus dynamics in soils receiving chemically treated dairy manure. *J. Environ. Qual.* **2004**, *33* (6), 2296−2305.

(14) Wong, J. W.; Selvam, A. Reduction of indicator and pathogenic microorganisms in pig manure through fly ash and lime addition during alkaline stabilization. *J. Hazard. Mater.* **2009**, *169* (1−3), 882.

(15) Farzadkia, M.; Mahvi, A. H. Comparison of extended aeration activated sludge process and activated sludge with lime addition method for biosolids stabilization. *Pak. J. Biol. Sci.* **2004**, *7* (12), 2061−2065.

DOI: 10.1021/acs.est.9b03269
Environ. Sci. Technol. 2020, 54, 1147−1156

(16) Ward, A. J.; Hobbs, P. J.; Holliman, P. J.; Jones, D. L. Optimisation of the anaerobic digestion of agricultural resources. *Bioresour. Technol.* **2008**, *99* (17), 7928−40.
(17) Carrere, H.; Antonopoulou, G.; Affes, R.; Passos, F.; Battimelli, A.; Lyberatos, G.; Ferrer, I. Review of feedstock pretreatment strategies for improved anaerobic digestion: From lab-scale research to full-scale application. *Bioresour. Technol.* **2016**, *199*, 386−397.
(18) Hansen, K. H.; Angelidaki, I.; Ahring, B. K. Anaerobic digestion of swine manure: inhibition by ammonia. *Water Res.* **1998**, *32* (1), 5−12.
(19) Ruike, W.; Higashimori, A.; Yaguchi, J.; Li, Y.-y. Use of real-time PCR with propidium monoazide for enumeration of viable *Escherichia coli* in anaerobic digestion. *Water Sci. Technol.* **2016**, *74* (5), 1243−1254.
(20) Anjum, R.; Grohmann, E.; Krakat, N. Anaerobic digestion of nitrogen rich poultry manure: Impact of thermophilic biogas process on metal release and microbial resistances. *Chemosphere* **2017**, *168*, 1637−1647.
(21) Wu, Y.; Cui, E.; Zuo, Y.; Cheng, W.; Rensing, C.; Chen, H. Influence of two-phase anaerobic digestion on fate of selected antibiotic resistance genes and class I integrons in municipal wastewater sludge. *Bioresour. Technol.* **2016**, *211*, 414−421.
(22) Feng, L.; Casas, M. E.; Ottosen, L. D. M.; M?ller, H. B.; Bester, K. Removal of antibiotics during the anaerobic digestion of pig manure. *Sci. Total Environ.* **2017**, *603*−*604*, 219−225.
(23) Qian, X.; Sun, W.; Gu, J.; Wang, X. J.; Zhang, Y. J.; Duan, M. L.; Li, H. C.; Zhang, R. R. Reducing antibiotic resistance genes, integrons, and pathogens in dairy manure by continuous thermophilic composting. *Bioresour. Technol.* **2016**, *220*, 425−432.
(24) Ho, Y. B.; Zakaria, M. P.; Latif, P. A.; Saari, N. Degradation of veterinary antibiotics and hormone during broiler manure composting. *Bioresour. Technol.* **2013**, *131* (131C), 476−484.
(25) Zhong, J.; Wei, Y.; Wan, H.; Wu, Y.; Zheng, J.; Han, S.; Zheng, B. Greenhouse gas emission from the total process of swine manure composting and land application of compost. *Atmos. Environ.* **2013**, *81* (2), 348−355.
(26) Fukumoto, Y.; Inubushi, K. Effect of nitrite accumulation on nitrous oxide emission and total nitrogen loss during swine manure composting. *Soil Sci. Plant Nutr.* **2009**, *55* (3), 428−434.
(27) Huang, R.; Tang, Y. Speciation dynamics of phosphorus during (hydro)thermal treatments of sewage sludge. *Environ. Sci. Technol.* **2015**, *49* (24), 14466−74.
(28) Huang, R.; Tang, Y. Evolution of phosphorus complexation and mineralogy during (hydro)thermal treatments of activated and anaerobically digested sludge: Insights from sequential extraction and P K-edge XANES. *Water Res.* **2016**, *100*, 439−447.
(29) Huang, R.; Fang, C.; Zhang, B.; Tang, Y. Transformations of Phosphorus Speciation during (Hydro)thermal Treatments of Animal Manures. *Environ. Sci. Technol.* **2018**, *52* (5), 3016−3026.
(30) Lu, X.; Berge, N. D. Influence of feedstock chemical composition on product formation and characteristics derived from the hydrothermal carbonization of mixed feedstocks. *Bioresour. Technol.* **2014**, *166*, 120−31.
(31) Idowu, I.; Li, L.; Flora, J. R.; Pellechia, P. J.; Darko, S. A.; Ro, K. S.; Berge, N. D. Hydrothermal carbonization of food waste for nutrient recovery and reuse. *Waste Manage.* **2017**, *69*, 480−491.
(32) Rafique, R.; Poulsen, T. G.; Nizami, A. S.; Asam, Z. U.; Murphy, J. D.; Kiely, G. Effect of thermal, chemical and thermo-chemical pre-treatments to enhance methane production. *Energy* **2010**, *35* (12), 4556−4561.
(33) Valo, A.; Carrere, H.; Delgenes, J. P. Thermal, chemical and thermo-chemical pre-treatment of waste activated sludge for anaerobic digestion. *J. Chem. Technol. Biotechnol.* **2004**, *79* (11), 1197−1203.
(34) He, C.; Giannis, A.; Wang, J. Y. Conversion of sewage sludge to clean solid fuel using hydrothermal carbonization: Hydrochar fuel characteristics and combustion behavior. *Appl. Energy* **2013**, *111*, 257−266.
(35) Escala, M.; Zumbühl, T.; Koller, C.; Junge, R.; Krebs, R. Hydrothermal carbonization as an energy-efficient alternative to established drying technologies for sewage sludge: A feasibility study on a laboratory scale. *Energy Fuels* **2013**, *27* (1), 454−460.
(36) APHA *Standard methods for the examination of water and wastewater*, 22nd ed.; In American Public Health Association/American Water Works Association/Water Environment Federation: Washington DC, USA, 2012.
(37) Hedges, J. I.; Stern, J. H. Carbon and nitrogen determinations of carbonate-containing solids. *Limnol. Oceanogr.* **1984**, *29* (3), 657−663.
(38) Okutman Tas, D.; Pavlostathis, S. G. Microbial Reductive Transformation of Pentachloronitrobenzene under Methanogenic Conditions. *Environ. Sci. Technol.* **2005**, *39* (21), 8264−8272.
(39) Misiti, T.; Tezel, U.; Pavlostathis, S. G. Fate and effect of naphthenic acids on oil refinery activated sludge wastewater treatment systems. *Water Res.* **2013**, *47* (1), 449−460.
(40) Cook, R. L.; Langford, C. H. Structural Characterization of a Fulvic Acid and a Humic Acid Using Solid-State Ramp-CP-MAS 13C Nuclear Magnetic Resonance. *Environ. Sci. Technol.* **1998**, *32* (5), 719−725.
(41) Vane, C. H.; Drage, T. C.; Snape, C. E.; Stephenson, M. H.; Foster, C. Decay of cultivated apricot wood (*Prunus armeniaca*) by the ascomycete *Hypocrea sulphurea*, using solid state ^{13}C NMR and off-line TMAH thermochemolysis with GC−MS. *Int. Biodeterior. Biodegrad.* **2005**, *55* (3), 175−185.
(42) Hedley, M. J.; Stewart, J. W. B. Method to measure microbial phosphate in soils. *Soil Biol. Biochem.* **1982**, *14* (4), 377−385.
(43) Murphy, J.; Riley, J. P. A modified single solution method for the determination of phosphate in natural waters. *Anal. Chim. Acta* **1962**, *27*, 31−36.
(44) Ortega-Martinez, E.; Zaldivar, C.; Phillippi, J.; Carrere, H.; Donoso-Bravo, A. Improvement of anaerobic digestion of swine slurry by steam explosion and chemical pretreatment application. Assessment based on kinetic analysis. *J. Environ. Chem. Eng.* **2016**, *4* (2), 2033−2039.
(45) Huang, W.; Zhao, Z.; Yuan, T.; Huang, W.; Lei, Z.; Zhang, Z. Low-temperature hydrothermal pretreatment followed by dry anaerobic digestion: A sustainable strategy for manure waste management regarding energy recovery and nutrients availability. *Waste Manage.* **2017**, *70*, 255−262.
(46) Bougrier, C.; Delgenès, J. P.; Carrère, H. Effects of thermal treatments on five different waste activated sludge samples solubilisation, physical properties and anaerobic digestion. *Chem. Eng. J.* **2008**, *139* (2), 236−244.
(47) Higgins, M. J.; Beightol, S.; Mandahar, U.; Suzuki, R.; Xiao, S.; Lu, H.-W.; Le, T.; Mah, J.; Pathak, B.; DeClippeleir, H.; Novak, J. T.; Al-Omari, A.; Murthy, S. N. Pretreatment of a primary and secondary sludge blend at different thermal hydrolysis temperatures: Impacts on anaerobic digestion, dewatering and filtrate characteristics. *Water Res.* **2017**, *122*, 557−569.
(48) Li, C.; Wang, X.; Zhang, G.; Yu, G.; Lin, J.; Wang, Y. Hydrothermal and alkaline hydrothermal pretreatments plus anaerobic digestion of sewage sludge for dewatering and biogas production: Bench-scale research and pilot-scale verification. *Water Res.* **2017**, *117*, 49−57.
(49) Wilson, C. A.; Novak, J. T. Hydrolysis of macromolecular components of primary and secondary wastewater sludge by thermal hydrolytic pretreatment. *Water Res.* **2009**, *43* (18), 4489−4498.
(50) Danso-Boateng, E.; Shama, G.; Wheatley, A. D.; Martin, S. J.; Holdich, R. G. Hydrothermal carbonisation of sewage sludge: Effect of process conditions on product characteristics and methane production. *Bioresour. Technol.* **2015**, *177*, 318−327.
(51) Li, Y.; Jin, Y.; Li, J.; Li, H.; Yu, Z. Effects of thermal pretreatment on the biomethane yield and hydrolysis rate of kitchen waste. *Appl. Energy* **2016**, *172*, 47−58.
(52) Wang, H.-Y.; Qian, H.; Yao, W.-R. Melanoidins produced by the Maillard reaction: Structure and biological activity. *Food Chem.* **2011**, *128* (3), 573−584.

DOI: 10.1021/acs.est.9b03269
Environ. Sci. Technol. 2020, 54, 1147−1156

(53) Yenigün, O.; Demirel, B. Ammonia inhibition in anaerobic digestion: A review. *Process Biochem.* **2013**, *48* (5−6), 901−911.
(54) Batstone, D. J.; Keller, J.; Angelidaki, I.; Kalyuzhnyi, S.; Pavlostathis, S.; Rozzi, A.; Sanders, W.; Siegrist, H.; Vavilin, V. The IWA anaerobic digestion model no 1 (ADM1). *Water Sci. Technol.* **2002**, *45* (10), 65−73.
(55) Pavlostathis, S., Kinetics and modeling of anaerobic treatment and biotransformation processes. In *Comprehensive Biotechnology, Environmental Biotechnology and Safety*, Agathos, S., Ed.; Elsevier: Amsterdam, The Netherlands, 2011; Vol. *6*.
(56) Pavlostathis, S.; Giraldo-Gomez, E. Kinetics of anaerobic treatment. *Water Sci. Technol.* **1991**, *24* (8), 35−59.
(57) Cimo, G.; Kucerik, J.; Berns, A. E.; Schaumann, G. E.; Alonzo, G.; Conte, P. Effect of heating time and temperature on the chemical characteristics of biochar from poultry manure. *J. Agric. Food Chem.* **2014**, *62* (8), 1912−8.
(58) Wang, L.; Li, A.; Chang, Y. Relationship between enhanced dewaterability and structural properties of hydrothermal sludge after hydrothermal treatment of excess sludge. *Water Res.* **2017**, *112*, 72−82.
(59) Gomez, X.; Diaz, M. C.; Cooper, M.; Blanco, D.; Moran, A.; Snape, C. E. Study of biological stabilization processes of cattle and poultry manure by thermogravimetric analysis and ^{13}C NMR. *Chemosphere* **2007**, *68* (10), 1889−97.
(60) Cao, X.; Ro, K. S.; Chappell, M.; Li, Y.; Mao, J. Chemical structures of swine-manure chars produced under different carbonization conditions investigated by advanced solid-state ^{13}C nuclear magnetic resonance (NMR) spectroscopy. *Energy Fuels* **2011**, *25* (1), 388−397.
(61) Amir, S.; Hafidi, M.; Merlina, G.; Hamdi, H.; Revel, J.-C. Elemental analysis, FTIR and 13C-NMR of humic acids from sewage sludge composting. *Agronomie* **2004**, *24* (1), 13−18.
(62) Conte, P.; De Pasquale, C.; Novotny, E. H.; Caponetto, G.; Laudicina, V. A.; Ciofalo, M.; Panno, M.; Palazzolo, E.; Badalucco, L.; Alonzo, G. CPMAS ^{13}C NMR characterization of leaves and litters from the reafforestated area of Mustigarufi in Sicily (Italy). *Open Magn. Reson. J.* **2010**, *3*, 89−95.
(63) Heilmann, S. M.; Molde, J. S.; Timler, J. G.; Wood, B. M.; Mikula, A. L.; Vozhdayev, G. V.; Colosky, E. C.; Spokas, K. A.; Valentas, K. J. Phosphorus Reclamation through Hydrothermal Carbonization of Animal Manures. *Environ. Sci. Technol.* **2014**, *48* (17), 10323−10329.
(64) Møller, H. B.; Sommer, S. G.; Ahring, B. K. Methane productivity of manure, straw and solid fractions of manure. *Biomass Bioenergy* **2004**, *26* (5), 485−495.
(65) Westerhoff, P.; Lee, S.; Yang, Y.; Gordon, G.; Hristovski, K.; Halden, R.; Herckes, P. Characterization, Recovery Opportunities, and Valuation of Metals in Municipal Sludges from U.S. Wastewater Treatment Plants Nationwide. *Environ. Sci. Technol.* **2015**, *49* (16), 9479.
(66) Hafidi, M.; Amir, S.; Revel, J.-C. Structural characterization of olive mill waster-water after aerobic digestion using elemental analysis, FTIR and 13C NMR. *Process Biochem.* **2005**, *40* (8), 2615−2622.
(67) De Pasquale, C.; Marsala, V.; Berns, A. E.; Valagussa, M.; Pozzi, A.; Alonzo, G.; Conte, P. Fast field cycling NMR relaxometry characterization of biochars obtained from an industrial thermochemical process. *J. Soils Sediments* **2012**, *12* (8), 1211−1221.
(68) Sambusiti, C.; Monlau, F.; Ficara, E.; Carrère, H.; Malpei, F. A comparison of different pre-treatments to increase methane production from two agricultural substrates. *Appl. Energy* **2013**, *104*, 62−70.
(69) Paul, S.; Dutta, A. Challenges and opportunities of lignocellulosic biomass for anaerobic digestion. *Resources, Conservation and Recycling* **2018**, *130*, 164−174.
(70) Phuttaro, C.; Sawatdeenarunat, C.; Surendra, K. C.; Boonsawang, P.; Chaiprapat, S.; Khanal, S. K. Anaerobic digestion of hydrothermally-pretreated lignocellulosic biomass: Influence of pretreatment temperatures, inhibitors and soluble organics on methane yield. *Bioresour. Technol.* **2019**, *284*, 128−138.
(71) Yang, B.; Tao, L.; Wyman, C. E. Strengths, challenges, and opportunities for hydrothermal pretreatment in lignocellulosic biorefineries. *Biofuels, Bioprod. Biorefin.* **2018**, *12* (1), 125−138.
(72) Hesselmann, R. P. X.; Rummell, R. V.; Resnlck, S. M. Anaerobic metabolism of bacteria performing enhanced biological phosphate removal. *Water Res.* **2000**, *34* (14), 3487−3494.
(73) Mino, T.; van Loosdrecht, M.C.M.; Heijnen, J.J. Microbiology and biochemistry of the enhanced biological phosphate removal process. *Water Res.* **1998**, *32* (11), 3193−3207.
(74) Fang, C.; Zhang, T.; Jiang, R.; Ohtake, H. Phosphate enhance recovery from wastewater by mechanism analysis and optimization of struvite settleability in fluidized bed reactor. *Sci. Rep.* **2016**, *6*, 32215.
(75) Hidalgo, D.; Corona, F.; Martín-Marroquín, J. M.; del Álamo, J.; Aguado, A. Resource recovery from anaerobic digestate: struvite crystallisation versus ammonia stripping. *Desalin. Water Treat.* **2016**, *57* (6), 2626−2632.
(76) Funke, A.; Ziegler, F. Hydrothermal carbonization of biomass: a summary and discussion of chemical mechanisms for process engineering. *Biofuels, Bioprod. Biorefin.* **2010**, *4* (2), 160−177.
(77) Huang, R.; Fang, C.; Lu, X.; Jiang, R.; Tang, Y. Transformation of Phosphorus during (Hydro)thermal Treatments of Solid Biowastes: Reaction Mechanisms and Implications for P Reclamation and Recycling. *Environ. Sci. Technol.* **2017**, *51* (18), 10284−10298.

DOI: 10.1021/acs.est.9b03269
Environ. Sci. Technol. 2020, 54, 1147−1156